

Neutrino dipole portal at electron colliders

Yu Zhang,¹ Mao Song,² Ran Ding,² and Liangwen Chen^{3,4,*}

¹*School of Physics, Hefei University of Technology, Hefei 230601, China*

²*School of Physics and Optoelectronics Engineering, Anhui University, Hefei 230601, China*

³*Institute of Modern Physics, CAS, Lanzhou 730000, China*

⁴*Advanced Energy Science and Technology Guangdong Laboratory, Huizhou 516000, China*

We propose to search for a heavy neutral lepton (HNL), that is also known as sterile neutrino, in electron colliders running with the center-of-mass energies at few GeV, including BESIII, Belle II, and the proposed Super Tau Charm Factory (STCF). We consider the HNL interacting with Standard Model neutrino and photon via a transition magnetic moment, the so-called dipole portal. We use the monophoton signature at electron colliders to probe the constraints on the active-sterile neutrino transition magnetic moments d as the function of the HNL's mass m_N . It is found that BESIII, Belle II and STCF can probe the upper limits for d down to $1.3 \times 10^{-5} \text{ GeV}^{-1}$, $8 \times 10^{-6} \text{ GeV}^{-1}$, and $1.3 \times 10^{-6} \text{ GeV}^{-1}$ with m_N around GeV scale, respectively, and have sensitivity to the previously unexplored parameter space for electron- (d_e) and tau-neutrino (d_τ) dipole portal with m_N from dozens to thousands MeV. On d_μ for HNL mixing with the muon-neutrino, Belle II and STCF can also provide leading constraints.

I. INTRODUCTION

The discovery of neutrino flavor oscillations confirms the existence of neutrino mass and mixing. This fact is one of the key observational facts indicating the imperfection of Standard Model (SM). Models containing new neutral fermionic states N , which can connect with neutrino masses via the so-called neutrino portal interaction, $\mathcal{L} \supset N H L$, have attracted significant attentions in the last few years. Here, N , so-called sterile neutrinos, is singlet under the SM gauge groups and often referred to as heavy neutral leptons (HNL), L is the SM leptons, and H is the Higgs doublet. The HNLs can mix with the left-handed neutrinos after the Higgs acquires a vacuum expectation value.

Alternatively, the heavy state N may couple to the SM through a higher-dimensional operator. In this work, we consider a HNL interacting with the SM via a transition magnetic moment, the so-called “neutrino dipole portal”, described by the following term in the Lagrangian:

$$\mathcal{L} \supset d_k \bar{\nu}_L^k \sigma_{\mu\nu} F^{\mu\nu} N + \text{H.c.}, \quad (1)$$

*Electronic address: chenlw@impcas.ac.cn

where $k = e, \mu, \tau$ denotes the flavor index of lepton, ν_L is a SM left-handed (active) neutrino field, $\sigma_{\mu\nu} = \frac{i}{2}[\gamma_\mu, \gamma_\nu]$, $F^{\mu\nu}$ is the electromagnetic field strength tensor, and d is the active-sterile neutrino transition magnetic moment, that controls the strength of the interaction with the units of $(\text{mass})^{-1}$.

A lot of attentions have been paid to the neutrino dipole portal, in the context of various laboratory, astrophysical, and cosmological bounds on d_k . A summary of existing constraints can be found in Refs.[1, 2], including Borexino [3, 4], Xenon-1T [4, 5], CHARM-II [6, 7], MiniBooNE [1, 8], LSND [1, 9], NOMAD [1, 10, 11], DONUT [12], LEP [1], and supernovae SN 1987A [1], BBN ^4He abundance [4], solar neutrinos [4, 13]. The sensitivities of future projects or estimated exclusions can also be obtained, such as SHiP [1], Forward LHC Detectors [14, 15], Icecube [7], SuperCDMS [16], DUNE [2], CE ν NS and E ν ES [17]. In this paper, we investigate the experimental sensitivity on active-sterile neutrino transition magnetic moments from electron colliders operated at the GeV scale, including BESIII [18], Belle II [19], and the proposed Super Tau Charm Factory (STCF) [20–22].

The rest paper is organized as follows. In Sec. II we describe the relevant signal and backgrounds at electron colliders. In Sec. III we summarize current constraints coming from existing experiments, and expected sensitivity on neutrino dipole coupling at BESIII, STCF and Belle II. Finally, a short summary is given in Sec. IV.

II. ELECTRON COLLIDER SIGNALS

In this work, we investigate the Dirac sterile neutrino N production via dipole portal at e^+e^- colliders that are operated with the center-of-mass (CM) energies of several GeV, such as BESIII, Belle II and future STCF. At these colliders, production will proceed via $e^+e^- \rightarrow \gamma^* \rightarrow N\bar{\nu}$ and $e^+e^- \rightarrow \gamma^* \rightarrow \bar{N}\nu$. The differential cross section for on-shell N and a SM neutrino production $e^+e^- \rightarrow N\bar{\nu}$ is

$$\frac{d\sigma_{N\bar{\nu}}}{dz_N} = \frac{d^2\alpha (s - m_N^2)^2 ((1 - z_N^2)s + (1 + z_N^2)m_N^2)}{4s^3}, \quad (2)$$

where α is the fine structure constant, $z_N \equiv \cos \theta_N$, with θ_N being the relative angle between electron beam axis and the momentum of N in the CM frame, s is the square of the CM energy, and m_N denotes the mass of N . Notice that the production rates of N associated with different flavor neutrino at electron collider are same, thus we omit the lepton flavor index of d here. The electron collider sensitivities on transition magnetic moments derived in this letter are equally applicable to all lepton flavor. The total production cross section for $e^+e^- \rightarrow N\bar{\nu}$ after integrating over all angles is

$$\sigma(e^+e^- \rightarrow N\bar{\nu}) = \frac{\alpha d^2 (s - m_N^2)^2 (s + 2m_N^2)}{3s^3}. \quad (3)$$

One can find that the production rate has little to do with the CM energy when $m_N \ll \sqrt{s}$. With the subsequent decay of $N \rightarrow \nu\gamma$, the signature to search is thus a single photon final state with missing energy, which exhibits a typical monophoton signature at e^+e^- colliders. The sterile neutrino N decays into a photon and a SM active neutrino through the dipole operator, with the decay rate given by

$$\Gamma_{N \rightarrow \nu\gamma} = \frac{|d|^2 m_N^3}{4\pi}. \quad (4)$$

To make sure that there exists visible photon in the final state, the subsequent decay of N must occur inside the fiducial volume of the detector. The probability of the heavy neutrino to decay radiatively in the fiducial volume after traveling a distance l from the primary vertex is given by

$$P_{dec}(l) = (1 - e^{-l/l_{dec}}) \text{Br}(N \rightarrow \nu\gamma). \quad (5)$$

l_{dec} is the decay length of N , which scales as

$$l_{dec} = c\tau\beta\gamma = \frac{4\pi}{|d|^2 m_N^4} \sqrt{E_N^2 - m_N^2}, \quad (6)$$

where E_N is the energy of N , with $E_N = \frac{s+m_N^2}{2\sqrt{s}}$ in the process $e^+e^- \rightarrow N\bar{\nu}$. It is assumed that the N decay is dominated by $N \rightarrow \nu\gamma$, hence the branching fraction $\text{Br}(N \rightarrow \nu\gamma) \simeq 1$ is taken in this work.

Then, the number of events in signal can be given as

$$N_s = L\sigma(e^+e^- \rightarrow N\nu)\text{Br}(N \rightarrow \nu\gamma)\epsilon_{cuts}\epsilon_{det}P_{dec}(l_D), \quad (7)$$

where l_D is the detector length, L is the luminosity of the monophoton data collected at electron colliders, ϵ_{cuts} and ϵ_{det} are the efficiencies of the kinematic cuts and detection for the final photon, respectively. Since N is usually produced on-shell and travels some distance before decaying, we employ the narrow width approximation to derive the kinematic information of the final state photon. The $1 - \cos\theta$ distribution is used for the photon from N decay, where θ is the photon angle in the rest frame of N [23, 24].

In the search for monophoton signature at electron colliders, the backgrounds can be classified into two categories: the irreducible background and the reducible background. The irreducible background arises from the neutrino production associated with one photon in SM $e^+e^- \rightarrow \nu\bar{\nu}\gamma$. The reducible background comes from a photon in the final state together with several other visible particles which cannot be detected due to limitations of the detector acceptance. We will discuss the reducible background later in details for each experiment, since it strongly depends on the detector performance.

A. Belle II

At Belle II, photons and electrons are able to be detected in the Electromagnetic Calorimeter (ECL), which covers a polar angle region of $(12.4 - 155.1)^\circ$ and has inefficient gaps between the endcaps and the

barrel for polar angles between $(31.4 - 32.2)^\circ$ and $(128.7 - 130.7)^\circ$ in the lab frame [25]. The reducible background for monophoton searches at Belle II comes from two major parts: one is mainly owing to the lack of polar angle coverage of the ECL near the beam direction, which is referred to as the “bBG”; the other one is mainly due to the gaps between the three segments in the ECL detector, which is referred to as the “gBG”[25]. The bBG arises from the electromagnetic processes $e^+e^- \rightarrow \gamma + \cancel{X}$ with \cancel{X} denoting the other particle (or particles) in the final state that are undetected due to the limitations of the detectors, dominated by $e^+e^- \rightarrow \gamma\gamma(\gamma)$ and $e^+e^- \rightarrow \gamma\ell^+\ell^-$, where except the detected photon all the other final state particles are emitted along the beam directions with $\theta > 155.1^\circ$ or $\theta < 12.4^\circ$ in the lab frame. At Belle II, we apply the detector cuts for the final detected photon (hereafter the “*basic cuts*”): $12.4^\circ < \theta_\gamma < 155.1^\circ$ in the lab frame.

For the asymmetric Belle II detector, in the bBG the maximum energy of the monophoton events in the CM frame, E_γ^m , is given by [27, 28] (if not exceeding $\sqrt{s}/2$)

$$E_\gamma^m(\theta_\gamma) = \frac{\sqrt{s}(A \cos \theta_1 - \sin \theta_1)}{A(\cos \theta_1 - \cos \theta_\gamma) - (\sin \theta_\gamma + \sin \theta_1)}, \quad (8)$$

where all angles are given in the CM frame, and $A = (\sin \theta_1 - \sin \theta_2)/(\cos \theta_1 - \cos \theta_2)$, with θ_1 and θ_2 being the polar angles corresponding to the edges of the ECL detector. To remove the above bBG, we adopt the detector cut

$$E_\gamma > E_\gamma^m \quad (9)$$

for the final monophoton (hereafter the “*bBG cut*”).

The monophoton energy in the gBG can be quite large in the central θ_γ region, since the gaps in the ECL are significantly away from the beam direction. The gBG have been simulated by Ref. [25] to search for an invisibly decaying dark photon. In Ref. [25], two different sets of detector cuts are designed to optimize the detection efficiency for different masses of the dark photon: the “*low-mass cut*” and “*high-mass cut*”. The “*low-mass cut*” can be described as $\theta_{\min}^{\text{low}} < \theta_\gamma^{\text{lab}} < \theta_{\max}^{\text{low}}$, where $\theta_{\min}^{\text{low}}$ and $\theta_{\max}^{\text{low}}$ are the minimum and maximum angles for the photon in the lab frame and can be respectively fitted as functions of [26]

$$\theta_{\min}^{\text{low}} = 5.399^\circ E_{\text{CM}}(\gamma)^2/\text{GeV}^2 - 58.82^\circ E_{\text{CM}}(\gamma)/\text{GeV} + 195.71^\circ, \quad (10)$$

$$\theta_{\max}^{\text{low}} = -7.982^\circ E_{\text{CM}}(\gamma)^2/\text{GeV}^2 + 87.77^\circ E_{\text{CM}}(\gamma)/\text{GeV} - 120.6^\circ, \quad (11)$$

with E_{CM} being the photon energy in the CM frame. The “*high-mass cut*” can be described as $\theta_{\min}^{\text{high}} < \theta_\gamma^{\text{high}} < \theta_{\max}^{\text{high}}$, where $\theta_{\min}^{\text{high}}$ and $\theta_{\max}^{\text{high}}$ can be respectively fitted as functions of [26]

$$\theta_{\min}^{\text{low}} = 3.3133^\circ E_{\text{CM}}(\gamma)^2/\text{GeV}^2 - 33.58^\circ E_{\text{CM}}(\gamma)/\text{GeV} + 108.79^\circ, \quad (12)$$

$$\theta_{\max}^{\text{low}} = -5.9133^\circ E_{\text{CM}}(\gamma)^2/\text{GeV}^2 + 54.119^\circ E_{\text{CM}}(\gamma)/\text{GeV} - 13.781^\circ. \quad (13)$$

To probe the sensitivity for active-sterile neutrino transition magnetic moments d , we define $\chi^2(d) \equiv S^2/(S+B)$, where S (B) is the number of events in the signal (background) processes. For background, $B = B_{\text{ir}} + B_{\text{re}}$ consists of the number of events in irreducible background B_{ir} and reducible background B_{re} . By solving $\chi^2(d_{95}) - \chi^2(0) = 2.71$, one can obtain the 95% confidence level (C.L.) upper limit for the neutrino dipole coupling d_{95} . Fig. 1 shows the limits under “*low-mass cut*” and “*high-mass cut*” with 50 ab^{-1} integrated luminosity. The number of events in irreducible background is calculated by integrating the differential cross sections under different detector cuts. In addition, the detection efficiency of photon ϵ_{dec} is assumed as 95% [25]. Following Refs. [29, 30], we take the detector length $l_D = 3 \text{ m}$ for Belle II. For the reducible background, it is found that about 300 (25000) gBG events survived the “*low-mass cut*” (“*high-mass cut*”) with 20 fb^{-1} integrated luminosity [25], which are rescaled according to the considered luminosity. We can see that the constraint with the “*low-mass cut*” is always better than the “*high-mass cut*” in the whole plotted mass region of N at Belle II.

In order to compare with other experiments where detailed simulations with gBG are not available, we also investigate the limits without taking gBG into account. In this scenario, the reducible background can be removed with the “*bBG cut*”, and now the background events all come from the irreducible backgrounds that survived the “*bBG cut*”. The 95% C.L. upper bound on d under the “*bBG cut*” with gBG omitted is shown in Fig. 1. It can be found that the upper bound under the “*bBG cut*” is about 4 times stronger than the one when gBG is considered under the “*low-mass cut*” with $0.3 \text{ GeV} \lesssim m_N \lesssim 9 \text{ GeV}$.

B. BESIII and STCF

At BESIII and STCF, we follow the cuts for photons applied by BESIII Collaboration (hereafter the “basic cuts”): $E_\gamma > 25 \text{ MeV}$ in the barrel ($|z_\gamma| < 0.8$) or $E_\gamma > 50 \text{ MeV}$ in the end-caps ($0.86 < |z_\gamma| < 0.92$) [31]. In the following, we use the BESIII detector parameters to analyze the constraints from STCF since these two experiments are similar. BESIII has not released any analysis on gBG to our knowledge, thus we neglect gBG in the monophoton reducible background at BESIII and STCF. In the BESIII and STCF analyses, the monophoton reducible background at the electron-positron colliders can be removed by applying the detector cut [32]:

$$E_\gamma > E_b(\theta_\gamma) = \frac{\sqrt{s}}{(1 + \sin \theta_\gamma / \sin \theta_b)}, \quad (14)$$

on the final state photon, where E_b is the maximum energy of the photon with the polar angle θ_b , and θ_b denotes the angle at the boundary of the sub-detectors. Taking into account the coverage of main drift chamber (MDC), electromagnetic calorimeter (EMC), and time-of-flight (TOF), we have the polar angel

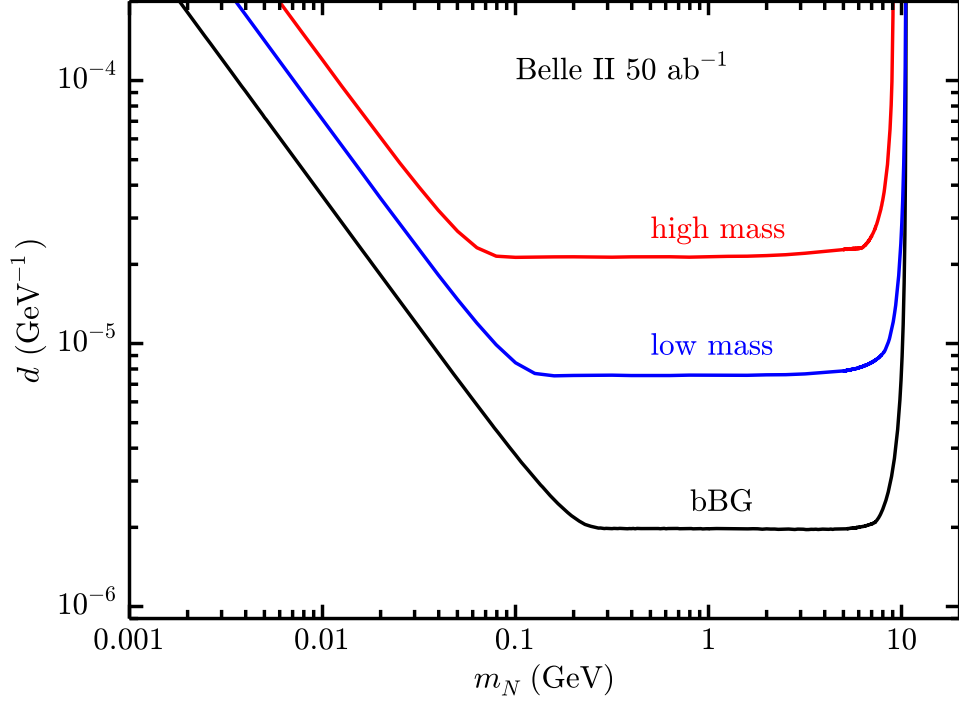


FIG. 1: The expected 95% C.L. upper limit on neutrino dipole coupling d at Belle II under “*low-mass cut*” (blue line), “*high-mass cut*” (red line) and “*bBG cut*” (black line), with 50 ab^{-1} integrated luminosity.

$\cos \theta_b = 0.95$ at BESIII [33]. In the following, we collectively refer to the “basic cuts” and cut (14) as the “advanced cuts”.

Since photon reconstruction efficiencies are all more than 99% [34] at BESIII, we take $\epsilon_{det} \simeq 100\%$ for the photon at BESIII and STCF in this work. The characteristic length scale of the detector is taken to be 80 cm, which is the outer radius of MDC at BESIII. Thus, we set the detector length $l_D = 0.8 \text{ m}$ for BESIII and STCF.

At BESIII the monophoton trigger has been implemented since 2012, and until now the corresponding events have been collected with the luminosity of about 28 fb^{-1} at the CM energy from 2.125 GeV to 4.95 GeV [35]. We compute the number of events due to signal (S) and backgrounds (B) under the “advanced cuts”, and define $\chi_{\text{tot}}^2(d) = \sum_i \chi_i^2(d)$, where $\chi_i^2(d) \equiv S_i^2/(S_i + B_i)$ for each BESIII colliding energy. We show the expected 95% C.L. upper limit on d with 28 fb^{-1} luminosity collected at BESIII in Figs. 2 and 3, which is obtained by demanding $\chi_{\text{tot}}^2(d_{95}) = \chi^2(0) + 2.71$. Fig. 2 also shows the expected limits on d with assumed 10 ab^{-1} luminosity at three different colliding energies in future STCF, respectively. One can find that, with same luminosity, operated at lower energy, STCF has better sensitivity in probing the low-mass region. This is because the monophoton cross section in small mass N production is not too dependent on

the CM energy, while decreases in the background with the increment of the CM energy.

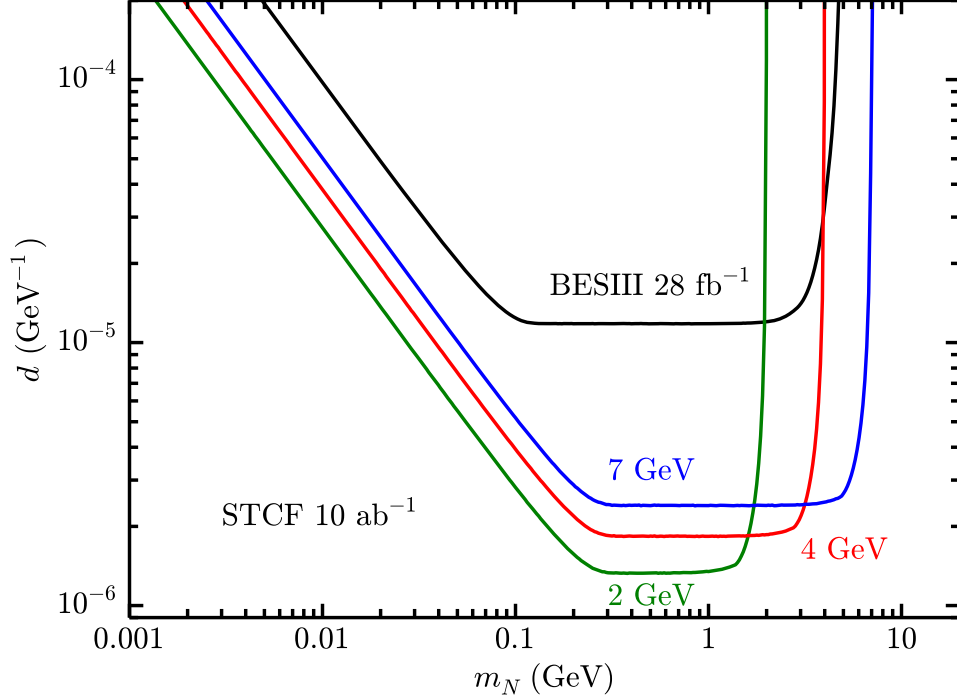


FIG. 2: The expected 95% C.L. upper bound on neutrino dipole coupling d at BESIII and STCF under "advanced cut". The limits from BESIII (black line) is obtained with about 28 fb^{-1} integrated luminosity collected at the various CM energies from 2.125 GeV to 4.95 GeV since 2012. The expected limits from STCF are shown at three typical energy points with 10 ab^{-1} integrated luminosity for $\sqrt{s} = 2$ (green line), 4 (red line), and 7 GeV (blue line), respectively.

III. RESULTS

The landscape of current constraints on transition magnetic moments are summarized in Fig. 3 with shaded region, coming from terrestrial experiments such as Borexino [4], Xenon-1T [4], CHARM-II [7], MiniBooNE [1], LSND [1], NOMAD [1, 10], DONUT [12], and LEP [1], and astrophysics supernovae SN 1987A [1]. It is noted that constraints on transition magnetic moments involving three SM active neutrinos ($\nu_{e,\mu,\tau}$) are similar in XENON-1T, Borexino, SN 1987A, and LEP [1, 4], which are shaded in gray.

For d_e , the constraint can also be from LSND [1], which is shown in orange region. The limits from CHARM-II [7], MiniBooNE [1], and NOMAD [1] are relevant only for d_μ , which are shown in skyblue regions. The constraint for d_μ also can be provided by LSND [1]. Since it is not competitive with CHARM-II, it is not shown here. DONUT [12] gave an upper 90% C.L. limit on d_τ of $5.8 \times 10^{-5} \text{ GeV}^{-1}$ for $m_N < 0.3 \text{ GeV}$, which is shown with pink curve.

In order to describe more intuitively, we summarize the sensitivity on d at 95% C.L. from the low-energy electron colliders, including Belle II, BESIII and STCF, which works for all the three neutrinos. The Belle II limit shown as solid curve in Fig. 3, has been analyzed taking into account the various SM backgrounds. With 50 ab^{-1} data, transition magnetic moment down to about $8 \times 10^{-6} \text{ GeV}^{-1}$ for mass about (0.1-7) GeV is expected to be probed by Belle II, which has better sensitivity than LEP [1]. A larger parameter space for d_e and d_τ in the mass region of 0.07-10 GeV and for d_μ in the mass region of 2-10 GeV is previously unconstrained by other experiments will be explored by Belle II. And for mass from about 3 GeV to 10 GeV, Belle II can still provide the most stringent restrictions on d_μ .

The STCF and BESIII limits, shown as dotted curves in Fig. 3, are obtained when the background due to the gaps in detectors is neglected. Using the monophoton signature with about 28 fb^{-1} luminosity collected at the CM energy from 2.125 GeV to 4.95 GeV during 2012-2020, the BESIII can probe the upper limit of d down to about $1.3 \times 10^{-5} \text{ GeV}^{-1}$ for $0.1 \text{ GeV} < m_N < 3 \text{ GeV}$, which is still competitive with LEP [1], and can provide better sensitivity for d_e and d_τ than existing experiments. With 30 ab^{-1} data at $\sqrt{s} = 4 \text{ GeV}$, STCF can provide constraints on transition magnetic moments $d \lesssim 1.3 \times 10^{-6} \text{ GeV}^{-1}$ for mass from 0.2 GeV to about 3 GeV. The expected limit from STCF running at 4 GeV with 30 ab^{-1} data can also give leading sensitivity on d_e and d_τ for mass $m_N \sim (0.07\text{-}3.8) \text{ GeV}$ and on d_μ for $m_N \sim (2\text{-}3.8) \text{ GeV}$.

The omission of the gBG in BESIII (28 fb^{-1}) leads to an almost comparable limit with Belle II (50 ab^{-1}) with gBG included for $m_N \lesssim 3 \text{ GeV}$. In order to compare the capability of probing the parameter space from different experiments, we also present a Belle II limit (dot-dashed curve) without gBG considered. It can be found that the luminosity of STCF is lower than Belle II, but STCF has better sensitivity in probing the low-mass region ($m_N \lesssim 3.5 \text{ GeV}$) than Belle II. This is because STCF is operated at a lower colliding energy where the monophoton cross section in SM is smaller than Belle II. About four times of magnitude difference in sensitivity between the two Belle II limits, the solid curve and the dot-dashed curve in Fig. 3 show that the control on gBG is important in probing the neutrino dipole portal.

IV. SUMMARY

In this paper, we analyzed the sensitivity on active-sterile neutrino transition magnetic moment d from several electron colliders operated at few GeV: Belle II, BESIII and STCF. With about 28 fb^{-1} luminosity in monophoton data collected during 2012-2020, the BESIII can provide the expected upper limit of d down to $1.3 \times 10^{-5} \text{ GeV}^{-1}$ for $0.1 \text{ GeV} < m_N < 3 \text{ GeV}$. Projected limits with Belle II and STCF experiments are also analyzed. Belle II with 50 ab^{-1} monophoton data can probe transition magnetic moment down to $8 \times 10^{-6} \text{ GeV}^{-1}$ for mass about (0.1-7) GeV, and will improve the sensitivity about four times with gBG

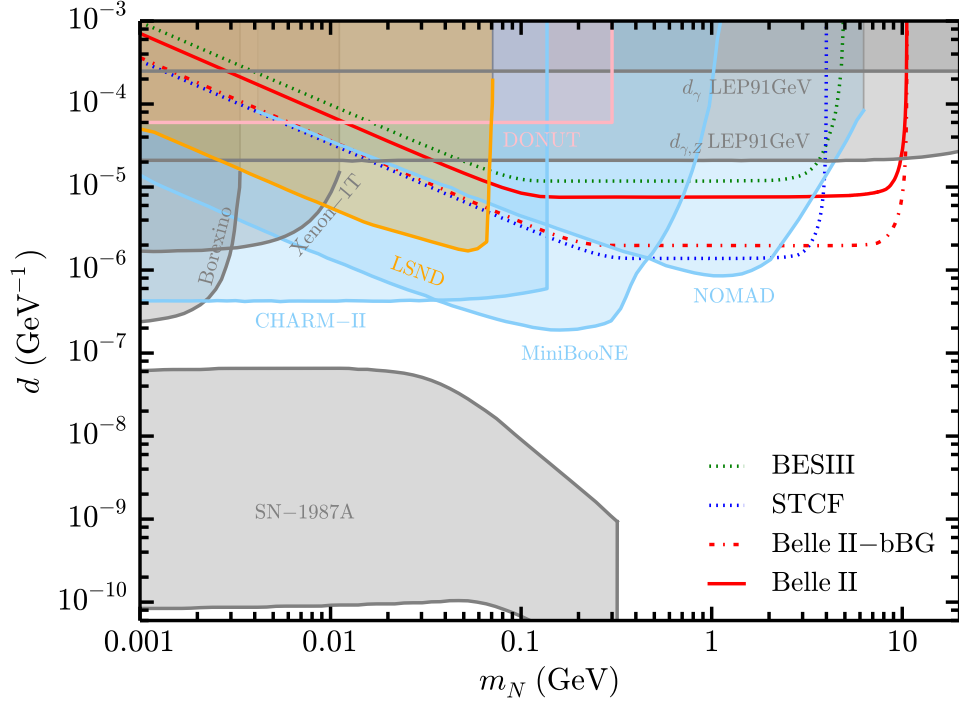


FIG. 3: The expected 95% C.L. exclusion limits on active-sterile neutrino transition magnetic moment d at Belle II, BESIII, and STCF, which work for all the three SM neutrinos. The Belle II limit (red solid line) is obtained under the “low-mass cut”, where both the bBG and the gBG are considered. The other Belle II limit (red dot-dashed line) is obtained with the “bBG cut” where the gBG is omitted. The BESIII limit (green dotted line) is obtained with the integrated luminosity of 28 fb^{-1} during 2012-2020 where the gBG is omitted. The STCF limits (blue dotted line) is obtained for $\sqrt{s} = 4 \text{ GeV}$ and 30 ab^{-1} under the “advanced cuts”, where the gBG is omitted. The landscape of current constraints are also presented with shaded region. The gray shaded regions exploiting the constraints from Borexino [4], Xenon1T [4], LEP [1], and SN-1987A [1] are relevant for all three SM neutrinos. The orange regions show the constraint on electron-neutrino dipole coupling d_e from LSND [1]. The skyblue regions show the constraints on muon-neutrino dipole coupling d_μ from CHARM-II [7], MiniBooNE [1], and NOMAD [1, 10]. The pink region shows the constraints on tau-neutrino dipole coupling d_τ from DONUT [12].

omitted. The future 4 GeV STCF with 30 ab^{-1} monophoton data can further improve the sensitivity to low-mass sterile neutrino ($m_N \lesssim 3.5 \text{ GeV}$) than Belle II. In general, BESIII, STCF and Belle II can explore the parameter space for d_e and d_τ , which is previously unconstrained by other existing experiments. And Belle II and STCF can also provide leading constraints on d_μ for high-mass sterile neutrino.

Acknowledgments

This work was supported in part by the National Natural Science Foundation of China (Grants No.12105327, No. 11805001) and the Key Research Foundation of Education Ministry of Anhui Province of China (No.KJ2021A0061).

-
- [1] G. Magill, R. Plestid, M. Pospelov and Y. D. Tsai, Phys. Rev. D **98** (2018) no.11, 115015 doi:10.1103/PhysRevD.98.115015 [arXiv:1803.03262 [hep-ph]].
 - [2] T. Schwetz, A. Zhou and J. Y. Zhu, JHEP **21** (2020), 200 doi:10.1007/JHEP07(2021)200 [arXiv:2105.09699 [hep-ph]].
 - [3] M. Agostini *et al.* [Borexino], Phys. Rev. D **96** (2017) no.9, 091103 doi:10.1103/PhysRevD.96.091103 [arXiv:1707.09355 [hep-ex]].
 - [4] V. Brdar, A. Greljo, J. Kopp and T. Opferkuch, JCAP **01** (2021), 039 doi:10.1088/1475-7516/2021/01/039 [arXiv:2007.15563 [hep-ph]].
 - [5] E. Aprile *et al.* [XENON], Phys. Rev. D **102** (2020) no.7, 072004 doi:10.1103/PhysRevD.102.072004 [arXiv:2006.09721 [hep-ex]].
 - [6] D. Geiregat *et al.* [CHARM-II], Phys. Lett. B **232** (1989), 539 doi:10.1016/0370-2693(89)90457-7
 - [7] P. Coloma, P. A. N. Machado, I. Martinez-Soler and I. M. Shoemaker, Phys. Rev. Lett. **119** (2017) no.20, 201804 doi:10.1103/PhysRevLett.119.201804 [arXiv:1707.08573 [hep-ph]].
 - [8] A. A. Aguilar-Arevalo *et al.* [MiniBooNE], Phys. Rev. Lett. **98** (2007), 231801 doi:10.1103/PhysRevLett.98.231801 [arXiv:0704.1500 [hep-ex]].
 - [9] C. Athanassopoulos *et al.* [LSND], Phys. Rev. Lett. **77** (1996), 3082-3085 doi:10.1103/PhysRevLett.77.3082 [arXiv:nucl-ex/9605003 [nucl-ex]].
 - [10] S. N. Gninenko and N. V. Krasnikov, Phys. Lett. B **450** (1999), 165-172 doi:10.1016/S0370-2693(99)00130-6 [arXiv:hep-ph/9808370 [hep-ph]].
 - [11] J. Altegoer *et al.* [NOMAD], Phys. Lett. B **428** (1998), 197-205 doi:10.1016/S0370-2693(98)00402-X [arXiv:hep-ex/9804003 [hep-ex]].
 - [12] R. Schwienhorst *et al.* [DONUT], Phys. Lett. B **513** (2001), 23-29 doi:10.1016/S0370-2693(01)00746-8 [arXiv:hep-ex/0102026 [hep-ex]].
 - [13] R. Plestid, doi:10.1103/PhysRevD.104.075027 [arXiv:2010.04193 [hep-ph]].
 - [14] K. Jodłowski and S. Trojanowski, JHEP **05** (2021), 191 doi:10.1007/JHEP05(2021)191 [arXiv:2011.04751 [hep-ph]].
 - [15] A. Ismail, S. Jana and R. M. Abraham, [arXiv:2109.05032 [hep-ph]].
 - [16] I. M. Shoemaker and J. Wyenberg, Phys. Rev. D **99** (2019) no.7, 075010 doi:10.1103/PhysRevD.99.075010 [arXiv:1811.12435 [hep-ph]].

- [17] O. G. Miranda, D. K. Papoulias, O. Sanders, M. Tórtola and J. W. F. Valle, [arXiv:2109.09545 [hep-ph]].
- [18] D. M. Asner, T. Barnes, J. M. Bian, I. I. Bigi, N. Brambilla, I. R. Boyko, V. Bytev, K. T. Chao, J. Charles and H. X. Chen, *et al.* Int. J. Mod. Phys. A **24** (2009), S1-794 [arXiv:0809.1869 [hep-ex]].
- [19] T. Abe *et al.* [Belle-II], [arXiv:1011.0352 [physics.ins-det]].
- [20] Q. Luo, W. Gao, J. Lan, W. Li and D. Xu, doi:10.18429/JACoW-IPAC2019-MOPRB031
- [21] A. E. Bondar *et al.* [Charm-Tau Factory], Phys. Atom. Nucl. **76** (2013), 1072-1085 doi:10.1134/S1063778813090032
- [22] X. D. Shi, X. R. Zhou, X. S. Qin and H. P. Peng, JINST **16** (2021) no.03, P03029 doi:10.1088/1748-0221/16/03/P03029 [arXiv:2011.01654 [physics.ins-det]].
- [23] L. F. Li and F. Wilczek, Phys. Rev. D **25** (1982), 143 doi:10.1103/PhysRevD.25.143
- [24] M. Masip, P. Masjuan and D. Meloni, JHEP **01** (2013), 106 doi:10.1007/JHEP01(2013)106 [arXiv:1210.1519 [hep-ph]].
- [25] E. Kou *et al.* [Belle-II], PTEP **2019** (2019) no.12, 123C01 [erratum: PTEP **2020** (2020) no.2, 029201] doi:10.1093/ptep/ptz106 [arXiv:1808.10567 [hep-ex]].
- [26] M. Duerr, T. Ferber, C. Hearty, F. Kahlhoefer, K. Schmidt-Hoberg and P. Tunney, JHEP **02** (2020), 039 doi:10.1007/JHEP02(2020)039 [arXiv:1911.03176 [hep-ph]].
- [27] J. Liang, Z. Liu, Y. Ma and Y. Zhang, Phys. Rev. D **102** (2020) no.1, 015002 doi:10.1103/PhysRevD.102.015002 [arXiv:1909.06847 [hep-ph]].
- [28] Y. Zhang, Z. Yu, Q. Yang, M. Song, G. Li and R. Ding, Phys. Rev. D **103** (2021) no.1, 015008 doi:10.1103/PhysRevD.103.015008 [arXiv:2012.10893 [hep-ph]].
- [29] A. Abashian *et al.* [Belle], Nucl. Instrum. Meth. A **479** (2002), 117-232 doi:10.1016/S0168-9002(01)02013-7
- [30] M. J. Dolan, T. Ferber, C. Hearty, F. Kahlhoefer and K. Schmidt-Hoberg, JHEP **12** (2017), 094 [erratum: JHEP **03** (2021), 190] doi:10.1007/JHEP12(2017)094 [arXiv:1709.00009 [hep-ph]].
- [31] M. Ablikim *et al.* [BESIII], Phys. Rev. D **96** (2017) no.11, 112008 doi:10.1103/PhysRevD.96.112008 [arXiv:1707.05178 [hep-ex]].
- [32] Z. Liu, Y. H. Xu and Y. Zhang, JHEP **06** (2019), 009 doi:10.1007/JHEP06(2019)009 [arXiv:1903.12114 [hep-ph]].
- [33] Z. Liu and Y. Zhang, Phys. Rev. D **99** (2019) no.1, 015004 doi:10.1103/PhysRevD.99.015004 [arXiv:1808.00983 [hep-ph]].
- [34] M. Ablikim *et al.* [BESIII], Phys. Rev. D **83** (2011), 112005 doi:10.1103/PhysRevD.83.112005 [arXiv:1103.5564 [hep-ex]].
- [35] <http://english.ihep.cas.cn/bes/doc/2250.html>